Synthesis of Pentasubstituted Pyridines

IV—Structural Characterization of the Addition Products of 1-(*N*,*N*-Diethylamine)prop-1-yne to *N*-Vinylcarbodiimides and -ketenimines†

Elvira Peláez-Arango, Miguel Ferrero and Fernando López-Ortiz*
Instituto Universitario de Química Organometálica Enrique Moles, Unidad Asociada al CSIC, Universidad de Oviedo, Oviedo, 33071 Spain

The reaction products of the addition of 1-(*N*,*N*-diethylamine)prop-1-yne to *N*-vinylcarbodiimides and -ketenimines have been identified. Two pyridine regioisomers can be obtained under thermal control according to a [4 + 2] or [2 + 2] cycloaddition mechanism. At temperatures above 100 °C a competing electrocyclic ring closure of the heterocumulene is observed. The structures of the pyridines isolated are assigned by a combination of HMBC and NOE difference spectra.

KEY WORDS NMR; ^{1}H NMR; ^{13}C NMR; pyridines cycloaddition; structure elucidation

INTRODUCTION

The synthesis of polysubstituted pyridines is an area of continuous interest owing to the broad range of applications of these compounds.[1] Among the available methods to build pyridine ring, those based on cycloaddition reactions are of the highest generality.[2] Their limitations are usually related to the periselectivity of the reaction and the accessible yields of the desired product.[3] We have recently shown[4] that the addition of ynamine **1** to *N*-vinylisothiocyanates **2** can be thermally controlled so that two different pentasubstituted pyridines, **3** and **4**, can be obtained in excellent yields (Scheme 1).

The formation of pyridines **3** and **4** can be explained by postulating a common intermediate compound derived from the initial [2 + 2] cycloaddition of ynamine **1** to the C=N double bond of the heterocumulene **2**.[5] It is known that heterocumulenes conjugated with a carbon–carbon double bond can act as 2π or 4π electron components in [2 + 2] and [4 + 2] cycloadditions,[3,6] respectively. In order to extend the scope of the method, a synthetic project has been carried out which includes the use of *N*-vinylcarbodiimides and -ketenimines as heterodienes in the reaction with ynamine **1**.[7] Here we report on the NMR characterization of the products obtained. On the basis of our previous experience,[4,5] the possible temperature dependence of the reaction has been taken into account. There are no generally valid rules that can be used *a priori* to predict which thermic pericyclic process should prevail.[8] Three different types of cycloadducts have been identified, and their structural assignment is based on the analysis of their 2D HMBC and NOE difference spectra.

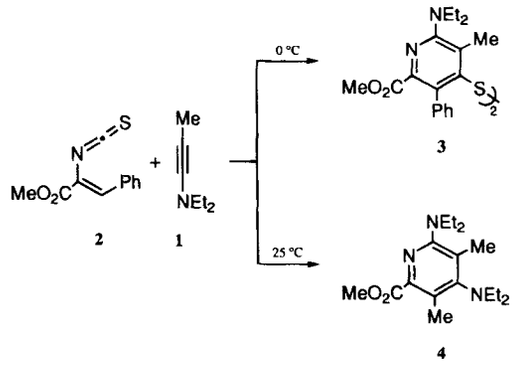

Scheme 1

* Author to whom correspondence should be addressed.
† Dedicated to Professor H. Günther on the occasion of his 60th birthday.

RESULTS AND DISCUSSION

Reaction of ynamine 1 with *N*-vinylcarbodiimides

The addition of ynamine **1** to carbodiimide **5a** in tetrahydrofuran (THF) or chloroform afforded pyridine **6a** when carried out at 0 °C, a mixture of regioisomers **6a** and **7a** at 25 °C in the same solvents or 100 °C in toluene, and a third reaction product **8a** when the temperature was raised to 140 °C in xylenes (Scheme 2). Isoquinoline **8a** (M^+ 278, 23%) is readily identified through the multiplicity pattern observed in the ^{1}H NMR spectrum. It results from the six-electron electrocyclic ring closure[9] of the starting carbodiimide involving the 2-azadiene moiety of the heterocumulene and a double bond of the phenyl ring substituent conjugated with it.

The mass spectrum of pyridine **6a** corresponds to the 1 : 1 adduct of a molecule of ynamine **1** plus one of cumulene **5a** (*m/z* 389, M^+ 55%). Accordingly, the ^{1}H and ^{13}C NMR spectra present the expected signals for this cycloadduct (Tables 1 and 2). As stated above,

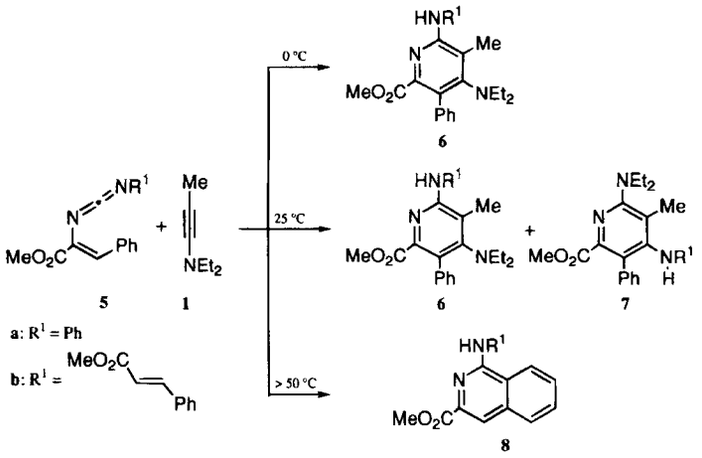

Scheme 2

electron-rich dienophiles might add to vinylheterocumulenes in a [2 + 2] or [4 + 2] way.[3,6] Furthermore, in each case two regioisomers are possible, the NMR spectra of which would be *a priori* very similar (Fig. 1).

The identification of the correct isomer was performed in two steps starting with the correlations observed in the HMBC spectrum for the methyl protons at 2.18 ppm. It shows cross peaks with the carbon atoms at 118.57, 153.82 and 157.03 ppm. Clearly, the highest field signal corresponds to the sp^2 carbon atom directly bonded to the CH_3 group. In addition, this carbon also correlates with the exchangeable proton at 6.36 ppm. The chemical shifts of the remaining two signals are in the expected range for sp^2 carbons bonded to nitrogen. The signal at 157.03 ppm further correlates with the quartet at 2.75 ppm arising from the methylene protons of the diethylamino group, which allows the assignment of this carbon as the one bonded to the NEt_2 substituent of the pyridine (Fig. 2).

These correlations are incompatible with the isomers **II** and **IV** depicted in Fig. 1 as possible structures for pyridine **6a**. The differentiation between the pair of regioisomers **I** and **III** is afforded by steady-state NOE experiments. The presaturation of the methylene protons at 2.75 ppm enhances the multiplet at 7.25 ppm assigned to the *ortho* protons of the phenyl ring substituent. This NOE clearly identifies the structure **I** as the reaction product obtained at 0 °C. The full assignment of the ^1H and ^{13}C NMR spectra is given in Tables 1 and 2, respectively.

As mentioned above, a mixture of two compounds, **6a** and **7a**, is obtained in a ratio of 9:1 when the reaction is carried out in THF or chloroform at 25 °C, and in a ratio of 1:1 if toluene is used at 100 °C. They were separated by column chromatography on silica gel. One of the components (the major one in the room-temperature run) corresponds to the pyridine **6a** previously determined. The assignment of the structure **III** (Fig. 1) to the new compound **7** is derived from the 2D HMBC spectrum. Thus, the methyl protons at 1.99 ppm present three cross peaks at 161.80, 147.65 and 117.47 ppm, which are assigned to the carbon atoms C-2, C-4 and C-3, respectively, of the pyridine ring following the same reasoning as outlined with pyridine **6a**. In this case, the NH proton at 5.56 ppm shows two correlations with the carbons at 117.54 and 122.61 ppm. The high-field signal further correlates with the *ortho* and

Table 1. Partial ^1H NMR assignments for compounds 6,[a] 7,[b] 10[c] and 11[d] [δ (ppm)]

Atom	6a	6b	7a	7b	10	11
H-8	3.55	3.49	3.58	3.57	3.54	3.48
H-9	6.36	6.42	3.32	2.73	3.15	5.77
H-10			1.19	0.96	1.11	
H-11		6.92	1.99	1.75	1.77	
H-12			5.56	5.90	5.68	
H-13		3.85				
H-14	2.18			6.93		2.29
H-15	2.75					2.71
H-16	0.91			3.77		0.87
H-17						
H-18		2.10				
H-19		2.66				
H-20		0.87				

[a] **6a**: 4-(*N*,*N*-Diethylamino)-6-methoxycarbonyl-3-methyl-5-phenyl-2-phenylaminopyridine.
[a] **6b**: 4-(*N*,*N*-Diethylamino)-2-(1-methoxycarbonyl-2-phenylethenyl)amino)-6-methoxycarbonyl-3-methyl-5-phenylpyridine.
[b] **7a**: 2-(*N*,*N*-Diethylamino)-6-methoxycarbonyl-3-methyl-5-phenyl-4-phenylaminopyridine.
[b] **7b**: 2-(*N*,*N*)-Diethylamino)-4(1-methoxycarbonyl-2-phenylethenyl)amino)-6-methoxycarbonyl-3-methyl-5-phenylpyridine.
[c] **10**: 2-(*N*,*N*-Diethylamino)-6-methoxycarbonyl-3-methyl-5-phenyl-4-diphenylmethylpyridine.
[d] **11**: 4-(*N*,*N*-Diethylamino)-6-methoxycarbonyl-3-methyl-5-phenyl-2-diphenylmethylpyridine.

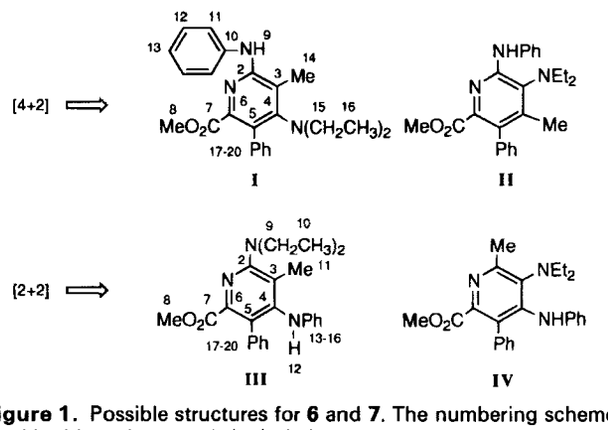

Figure 1. Possible structures for **6** and **7**. The numbering scheme used in this assignment is included.

Table 2. ^{13}C NMR assignments for compounds 6a and b, 7a and b, 10 and 11 [δ (ppm)]

Atom	6a	6b	7a	7b	10	11
C-2	157.03	153.12	161.80	161.70	162.17	160.54
C-3	118.57	118.02	117.47	114.03	127.30	132.39
C-4	153.82	157.32	147.65	147.38	150.99	156.56
C-5	127.45	127.35	122.61	120.90	131.00	132.36
C-6	146.23	146.07	144.81	143.90	145.12	143.50
C-7	167.89	167.34	167.79	167.63	168.07	167.98
C-8	51.86	52.44	51.94	51.75	51.86	51.78
C-9	—		44.56	44.20	45.07	55.45
C-10	141.22	129.12	13.40	13.22	13.31	142.64
C-11	118.52	121.35	16.87	16.91	18.22	129.59
C-12	128.78	167.05	—		52.31	127.25
C-13	121.42	51.69	143.40	128.46	141.12	126.18
C-14	14.04	134.79	117.54	118.56	129.14	15.33
C-15	46.34	128.77	129.45	166.10	128.09	46.33
C-16	13.76	128.27	121.17	52.50	126.12	13.75
C-17	137.34	127.77	135.10	133.26	137.62	137.51
C-18	127.64	13.91	129.03	128.95	129.42	128.04
C-19	129.85	46.12	127.79	127.52	127.73	130.02
C-20	126.94	13.72	128.73	127.88	128.21	127.90
C-21		137.32		135.67		
C-22		129.91		128.78		
C-23		127.58		129.23		
C-24		126.90		127.71		

para protons of the *N*-phenyl ring, and is therefore assigned to the *ortho* carbon of this substituent. The long-range correlation H(*ortho*)–C(*ortho*) arises from the symmetry of the ring.[10] Consequently, the signal at 122.61 ppm identifies the carbon C-5 of the pyridine heterocycle (Fig. 3). These data are only compatible with structure **III** for pyridine **7a**. The assignment is further supported by the NOEs produced on the *ortho* protons of both types of phenyl rings of the molecule when the NH signal is saturated.

The products obtained indicate that the reaction proceeds regioselectively through a [4 + 2] mechanism at 0 °C, which competes with the [2 + 2] cycloaddition when the reaction is performed at 25 °C (9 : 1) or 100 °C (1 : 1) (Scheme 3). This suggests that at higher temperatures the [2 + 2] process should be largely favoured. However, this cannot be fully confirmed because at 140 °C the heterocumulene reacts through an electrocyclic ring closure.

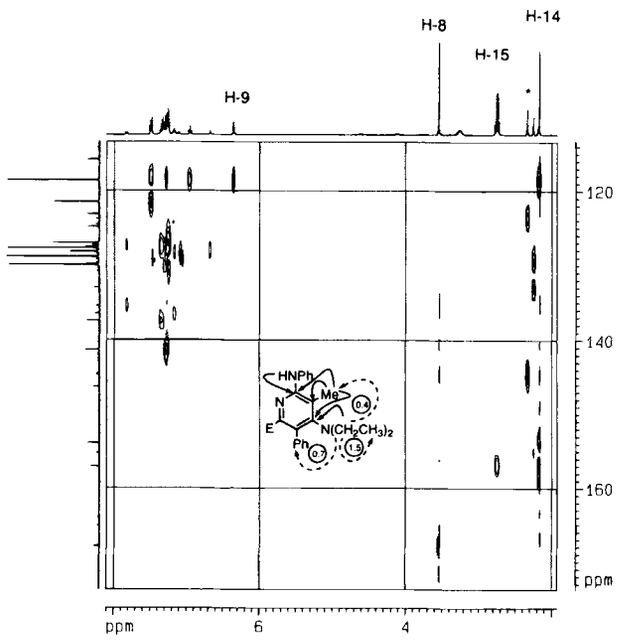

Figure 2. Section of the 400 MHz proton-detected HMBC spectrum in $CDCl_3$ for **6a**. Continuous arrows on the formula correspond to key correlations discussed in the text. Selected NOEs are indicated by dashed arrows and circled figures express the percentage of enhancement.

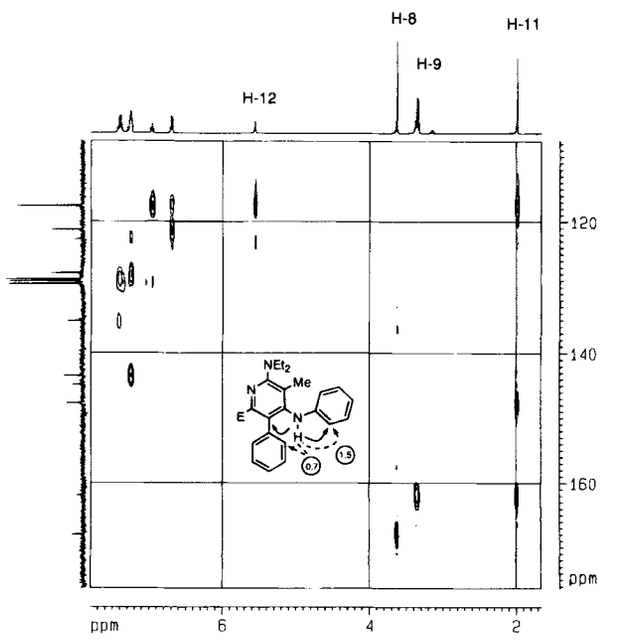

Figure 3. Proton detected (400 MHz) HMBC spectrum in $CDCl_3$ for **7a**. Continuous arrows on the formula correspond to key correlations discussed in the text. Selected NOEs are indicated by dashed arrows and circled figures express the percentage of enhancement.

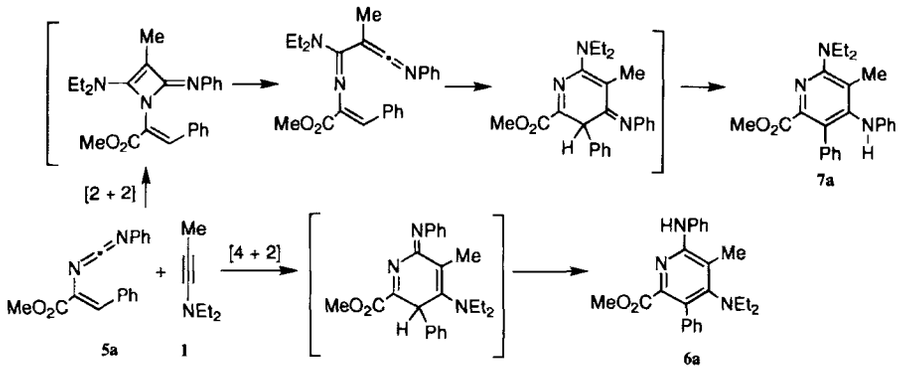

Scheme 3

This limitation is overcome when carbodiimide **5b** is used as the heterocumulene. At 0 °C the addition of ynamine **1** affords regioselectively the [4 + 2] cycloadduct **6b**, whereas at 100 °C the pyridine **7b** derived from the initial [2 + 2] cycloadditions is exclusively obtained (Scheme 2). The identification of these compounds was achieved in the same way as described for **6a** and **7a** (Tables 1 and 2). The NOE difference experiments also allowed the stereochemistry of the *N*-vinyl substituent to be established. A selection of the most significant NOEs found for pyridines **6b** and **7b** are summarized in Fig. 4.

Reaction of ynamine 1 with *N*-vinylketenimines

The addition of ynamine **1** to ketenimine **9** resembles that of carbodiimides **5**. At 0 °C it affords only one compound, pyridine **10**, whereas at 25 °C a mixture of the two pyridine regioisomers **10** and **11** is obtained. Their relative proportion was 1.1 : 1 and they were separated by column chromatography using diethyl ether–hexane (1 : 1, v/v) as eluent. Again, at higher temperatures (above 50 °C) the electrocyclic ring closure of the heterocumulene is favoured over the cycloaddition reaction and isoquinoline **12** is isolated (Scheme 4). The identification of **12** is trivial and will not be discussed.

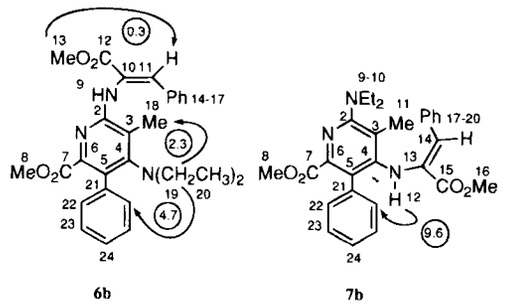

Figure 4. Structural formulae of **6b** and **7b**. Selected NOEs are identicated by arrows.

Substantially, the temperature dependence of the regioselectivity of the process is now reversed when compared with that of the analogous reaction with carbodiimides **5**. Their structural elucidation can be made through the analysis of the correlations in the HMBC spectra of the methyl and methyne protons with the carbons separated by two and/or three bonds.

As expected, the CH_3 protons show three cross peaks corresponding to the same molecular fragment of both pyridines **10** and **11**. Therefore, they cannot be assigned to any specific regioisomer. The identification is finally achieved when the previous information is complemented with the correlations of the $CHPh_2$ substituent. For pyridine **10** this proton appears at 5.68 ppm and exhibits five cross peaks at 127.30, 129.14, 131.00, 141.12 and 150.99 ppm [Fig. 5(b)]. Significantly, the signal at 131.00 ppm additionally correlates with the *ortho* protons of the phenyl ring substituent of the pyridine, a situation only possible if this carbon is C-5 in the regioisomer **10** (see Scheme 4 for the numbering used).

On the other hand, the proton of the $CHPh_2$ group of pyridine **11** absorbs at 5.77 ppm and correlates with four carbons at 129.59, 132.36, 142.64 and 160.54 ppm

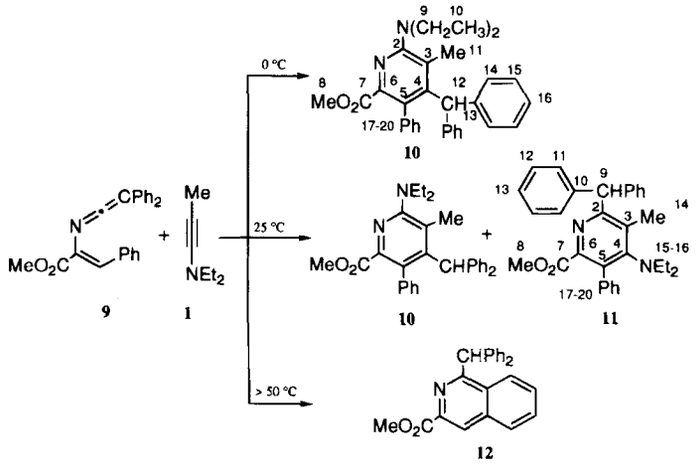

Scheme 4

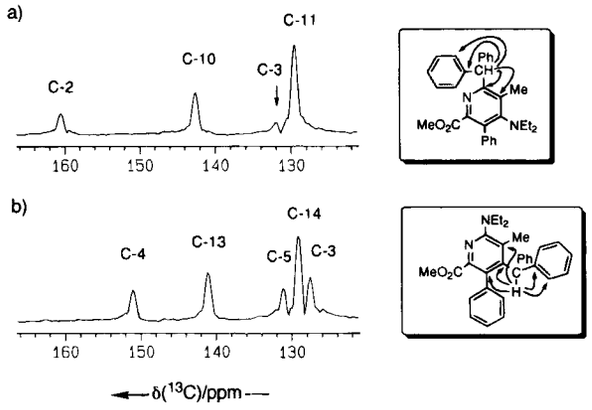

Figure 5. Columns extracted from the 2D HMBC spectra of **10** and **11** at the chemical shift of the $CHPh_2$ proton: (a) pyridine **10**, 5.77 ppm; (b) pyridine **11**, 5.68 ppm. See text for discussion.

[Fig. 5(a)]. The quaternary carbon atoms at 132.36 and 160.54 ppm also correlate with the methyl protons, and the signals at 129.59 and 142.64 ppm are easily identified as the C-*ortho* and C-*ipso*, respectively, of the phenyl ring bonded to the CH because of their correlations with other aromatic protons. This model of connectivity is only consistent with pyridine **11**. All other signals are straightforwardly assigned (Tables 1 and 2) following the same analysis as developed for pyridines **3** and **4**.

CONCLUSIONS

The addition of ynamine **1** to the *N*-vinylcarbodiimides **5** and -ketenimines **9** affords two pyridine regioisomers. Depending of the temperature of the reaction and the substitution pattern of the heterocumulene, the product arising from the initial [4 + 2] or [2 + 2] cycloaddition mechanism can be obtained regioselectively. In borderline situations the resulting mixtures are easily separated by column chromatography. A competing electrocyclic ring closure process is observed for heterocumulenes **5** and **9** at temperatures above 140 °C and 50 °C, respectively. The pyridines isolated have been unequivocally identified and their ^1H and ^{13}C NMR spectra fully assigned on the basis of HMBC and NOE difference spectra.

EXPERIMENTAL

NMR spectra were recorded on a Bruker AMX 400 spectrometer operating at 400.13 and 100.61 MHz for ^1H and ^{13}C, respectively, using a 5 mm broadband reverse probe. $CDCl_3$ was used as solvent and chemical shifts were referenced internally to TMS. Relevant parameters were as follows: pulse widths, 4.8 μs (45°, ^1H) and 5.1 μs (45°, ^{13}C) at an attenuation level of 3 dB in both cases; sweep width, 4 kHz (^1H) and 20–27 kHz (^{13}C); number of scans, 16 (^1H) and 512 (^{13}C); and computer memory, 32K. NOE experiments were performed on samples degassed by several freeze–thaw cycles. Each line of the target multiplet was included in a frequency list and individually pre-irradiated[11] for 0.2 s with a power attenuation of 85 dB. The process was repeated cyclically to afford a total saturation of 6 s. A 90° read pulse yielded the FID, which was weighted with an exponential function of line broadening factor 0.3 Hz. Two-dimensional HMQC and HMBC spectra were measured with the standard pulse sequences and the parameters used were similar to those reported previously.[5]

REFERENCES

1. F. S. Yates, in *Comprehensive Heterocyclic Chemistry*, edited by A. R. Katritzky, C. W. Rees, A. J. Boulton and A. McKillop, Vol. 2, Chapt. 2.09, pp. 511–521. Pergamon Press, Oxford (1984).
2. D. L. Boger and S. M. Weinreb, *Hetero Diels–Alder Methodology in Organic Synthesis*. Academic Press, New York (1987); R. Gompper and H. Heinemann, *Angew. Chem., Int. Ed. Engl.* **19**, 217 (1980); J. Barluenga, F. J. González, R. Péréz-Carlón and S. Fustero, *J. Org. Chem.* **56**, 6751 (1991), and references cited therein.
3. A. Dondoni, L. Kniezo and A. Medici, *J. Org. Chem.* **47**, 3994 (1982).
4. J. Barluenga, M. Ferrero, E. Peláez-Arango, F. López-Ortiz and F. Palacios, *J. Chem. Soc., Chem. Commun.* 865 (1994).
5. E. Peláez-Arango, F. López-Ortiz, J. Barluenga, M. Ferrero and F. Palacios, *Magn. Reson. Chem.* **32**, 646 (1994).
6. R. Fuks, *Tetrahedron* **26**, 2161 (1970); K. Takaki, A. Okamura, Y. Ohshiro and T. Agawa, *J. Org. Chem.* **43**, 402 (1978); K. Hafner, J. Häring and W. Jäkel, *Angew. Chem., Int. Ed. Engl.* **9**, 217 (1980); L. Kniezo, P. Kristian, J. Imrich, F. Ugozzoli and D. Andreetti, *Tetrahedron* **44**, 543 (1988).
7. J. Barluenga, M. Ferrero and F. Palacios, *Synlett.* submitted for publication; M. Ferrero, Doctoral Thesis, Oviedo (1992).
8. J. S. Burnier and W. L. Jorgensen, *J. Org. Chem.* **49**, 3001 (1984); M. Giffard and J. Cousseau, *J. Chem. Res.* (*S*) 300 (1985).
9. T. L. Gilchrist, G. E. Gymer and C. W. Rees, *J. Chem. Soc., Chem. Commun.* 835 (1973); L. E. Overman and S. Tsuboi, *J. Am. Chem. Soc.* **99**, 2813 (1977); I. Hassan and F. W. Fowler, *J. Am. Chem. Soc.* **100**, 6696 (1978).
10. J. Barluenga, R. Pérez-Carlón, J. González, J. Joglar, F. López-Ortiz and S. Fustero, *Bull. Soc. Chim. Fr.* **129**, 566 (1992); J. Kawabata, E. Fukushi, M. Hara and J. Mizutami, *Magn. Reson. Chem.* **30**, 6 (1992).
11. M. Kinns and J. K. M. Sanders, *J. Magn. Reson.* **56**, 518 (1984).